ELSEVIER

Journal of Organometallic Chemistry 488 (1995) 99–108

Journal of Organometallic Chemistry

Water-soluble organometallic compounds. 5. [☆] The regio-selective catalytic hydrogenation of unsaturated aldehydes to saturated aldehydes in an aqueous two-phase solvent system using 1,3,5-triaza-7-phosphaadamantane complexes of rhodium [☆☆]

Donald J. Darensbourg [a,*], Nicole White Stafford [a], Ferenc Joó [b], Joseph H. Reibenspies [a]

[a] *Department of Chemistry, Texas A & M University, College Station, TX 77843, USA*
[b] *Institute of Physical Chemistry, Kossuth Lajos University, Debrecen, H-4010, Hungary*

Received 6 June 1994

Abstract

The water-soluble phosphine complex of Rh(I), [Rh(PTAH)(PTA)$_2$Cl]Cl (**1**), has been synthesized from $RhCl_3$ and 1,3,5,-triaza-7-phosphaadamantane (PTA) in 96% ethanol. This complex is an effective catalyst for the regioselective reduction of unsaturated aldehydes to saturated aldehydes. The rate of hydrogenation of *trans*-cinnamaldehyde with sodium formate as reductant was studied as a function of catalyst, substrate, and sodium formate concentration. The presence of an excess of PTA was found to inhibit hydrogenations completely. This reaction was also found to be partially inhibited by cyclo-octatetraene and Hg(0), leading to the conclusion that both heterogeneous and homogeneous mechanisms are operating. Recycling experiments show complex **1** to be quite robust, with minimal leaching into the organic phase in a biphasic system. The complex resulting from the addition of an excess of PTA to **1**, [Rh(PTAH)$_3$(PTA)Cl]Cl$_3$ (**2**), has been prepared and structurally characterized by a single crystal X-ray diffraction study. ^{31}P and ^{1}H NMR, IR, and UV-VIS spectroscopy and pH titrametric measurements were employed to study the reactivity of the various rhodium PTA complexes in aqueous solutions.

Keywords: Rhodium; Hydrogenation; Crystal structure

1. Introduction

Homogeneous catalysts have many advantages over their heterogeneous counterparts. These include a better defined active site, generally higher activities and selectivities, lower operating temperatures and pressures, and the ability to tailor steric and electronic properties (and consequently catalytic properties) [2,3]. However, engineering difficulties have prevented industrial utilization of many advances in this field in large-scale syntheses [3]. The high cost and toxicity of the transition metals involved, requires their recovery from product and recirculation [4]. Therefore, industrially applicable homogeneous catalysts need to be easily separable from reaction products without concomitant deactivation [2–4]. Research beginning in the late 1960s has been directed towards combining the advantages of both systems by "heterogenizing" homogeneous catalysts [3]. Some of the areas most explored are the fixation of metal complexes on solid supports [3,5], the use of colloidal dispersions [6], and biphasic catalysis [4,7].

The presence of unperceived metal colloids in "homogeneous" catalysts has often received inadequate attention, because of difficulties in the detection of the colloids and the reproducibility of experiments [8]. However, the utility and often high activities of such systems has resulted in growing interest in catalysis by finely dispersed metal colloids [9]. Aqueous colloidal dispersions can be prepared in the presence of reagents that afford steric or electrosteric stabilization, such as polymers and surfactants [9c–9e]. These colloids are

☆ For IV, see ref. [1].
☆☆ Dedicated to Prof. Fausto Calderazzo on the occasion of his 65th birthday.
* Corresponding author.

SSDI 0022-328X(94)00024-7

typically used for the catalytic hydrogenation of olefinic groups [9c,9d]. For example, colloidal suspensions of rhodium particles have been prepared by reducing rhodium trichloride with sodium borohydride in the presence of surface active trisulfonated compounds, (see, for example, **A**) [6c]. These colloids are very stable towards aggregation and are active catalysts for

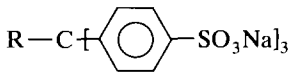

$R = C_{17}H_{37}; C_{16}H_{33}; C_9H_{19}.$ **(A)**

the hydrogenation of alkenes under biphasic conditions. The combining of techniques to facilitate the recycling of highly active catalysts is also seen in the immobilization of protected metal colloids for heterogeneous catalysis [10].

In a biphasic system two immiscible liquids are used to facilitate the separation of product(s) from the catalyst. Typically, an organic layer contains the substrate and product(s) and an aqueous layer contains the catalyst. The two layers are brought into contact in the interface region, and the reaction can occur in either layer or at the interface [11]. In order to utilize an aqueous biphasic system, the catalyst must be soluble and stable in water, a condition not met by most homogeneous catalysts. Unfortunately, most organometallic compounds are very moisture sensitive, and decompose in the presence of water to form metal oxides and hydroxides [12]. However, use of water as a solvent, if possible, has advantages. It is economical, non-toxic, and environmentally acceptable, and can exert a positive influence on regioselectivity and activity [11,13].

Solubility of transition metal complexes in aqueous media is usually accomplished by the attachment of charged or polar substituents (e.g. $-SO_3H$, -COOH, -OH, $-NH_2$, $-PO_3H_2$) to phosphines [7a,7b]. Electrostatic forces are also important in solubilizing highly charged complex ions in water. The most widely studied water-soluble complexes are those containing the sulfonated phosphines, e.g., *meta*-sulphonatophenyldiphenylphosphine (TPPMS) and tris-*meta*-sulphonatophenylphosphine (TPPTS) [7a,7b]. The rhodium complex with TPPTS is used in the biphasic hydroformylation of propylene to butyraldehyde; production is currently at 300,000 tons per year [14,15]. Aqueous biphasic systems can also be used in hydrogenation [7a,7b,11,16], carbonylation [17,18] isoprenylation [15,18], and asymmetric synthesis [19]. The development of this field is also important for the biological sciences. Water-soluble catalysts can be used to alter biomembrane fluidity [20], as biomimetic models [21], and in the development of new pharmaceuticals [22].

In 1974, Daigle et al. synthesized the water-soluble phosphine 1,3,5-triaza-7-phosphaadamantane (PTA) and its oxide (PTAO) and methyl-ammonium (PTA-Me^+) derivatives [23]. This ligand was subsequently shown to form stable complexes with Group 6 metal carbonyls [24] and mercury salts [25]. Recently PTA has been used in the development of water-soluble catalysts [1,26]. Preliminary results from that study indicated that $RuCl_2(PTA)_4$ and $RhCl(PTA)_3$ (**1**) catalytically hydrogenate the aldehyde and the olefin functions, respectively, of unsaturated aldehydes with a high degree of selectivity. The ruthenium hydrogenation process was described in detail in the fourth paper on this series [1]. In this paper, we report on the synthesis, structure and reactivity of the rhodium PTA complexes, $[Rh(PTAH)(PTA)_2Cl]Cl$ (**1**) and $[Rh(PTAH)_3(PTA)Cl]Cl_3$ (**2**), and on the mechanism of hydrogenation of olefins by **1**.

2. Experimental details

2.1. Materials and methods

All reactions were carried out under an inert atmosphere with degassed solvents. Solution IR spectra were taken in a 0.015 mm CaF_2 cell on a Mattson 6020 spectrometer. NMR spectra were collected using both Varian XL-200E (^{13}C and ^1H) and Varian XL200 (^{31}P) spectrometers in D_2O. pH titrations were carried out with a PHM 84 pH-meter, ABU 80 Autoburette and TTT 60 Titrator of Radiometer and an OP-08080 Radelkis pH-sensitive glass electrode. ICP measurements were made on a Spectroflame ICP, $\lambda = 249.077$ nm, Ar plasm, 1.2 kW. All chemicals were obtained commercially without further purification.

2.2. Synthesis of [Rh(PTAH)(PTA)$_2$Cl]Cl (1)

This complex was prepared as previously described [26]. A solution of 500 mg of $RhCl_3 \cdot 3H_2O$ in 25 ml of 96% ethanol was added to a stirred hot solution of 1.89 g PTA in 65 ml of 96% ethanol under nitrogen. A light yellow precipitate separated almost immediately, and did not change color during a subsequent 2 reflux. The mixture was filtered while warm, and the yellow powder washed with ethanol and acetone. Yield of $[Rh(PTAH)(PTA)_2Cl]Cl$: 1274 mg (98%). Its ^1H NMR spectrum exhibited two broad singlets at 4.5 ppm and 4.2 ppm, which correspond respectively to the methylene unit between two nitrogens and that between a nitrogen and a phosphorus. Two broad phosphorus resonances were observed in the ^{31}P NMR spectrum at -21 ppm and -23 ppm. Anal. Calc. for $C_{18}H_{37}N_9P_3Cl_2Rh$: C, 33.45; H, 5.95; Cl, 10.97. Found: C, 32.93; H, 6.48; Cl, 11.48%. Recrystallization of **1** from 0.1 M HCl provided X-ray quality crystals of $[Rh(PTAH)_2Cl_2]Cl$ in almost quantitative yield.

2.3. Synthesis of $[Rh(PTAH)_3(PTA)Cl]Cl_3$ (2)

Dissolution of 61 mg of $Rh(PTA)_3Cl$ (0.1 mmol) and 32 mg of PTA (0.2 mmol) in 1 ml of deoxygenated water gave a clear golden-yellow solution. Degassed acetone (2 ml) was layered on top of the aqueous solution. The solution turned deep red within 24 h and after several days large red crystals were isolated in almost quantitative yield. ^{31}P NMR δ: −21.6 (dt, $J_{Rh-P} = 107$ Hz, $J_{P-P} = 23$ Hz), δ: −49.2 (dt, $J_{Rh-P} = 80$ Hz, $J_{P-P} = 23$ Hz).

2.4. X-ray structural determination of $[Rh(PTAH)_3(PTA)Cl]Cl_3$ (2)

A red parallelepiped (0.2 mm × 0.34 mm × 0.36 mm) was mounted on a glass fiber with epoxy cement at room temperature and cooled to 193 K in a N_2 cold stream. Preliminary examination and data collection were performed on the same Nicolet R3m/V X-ray diffractometer [27a]. Cell parameters were calculated from the least-squares fitting of the setting angles for 25 reflections. ω scans for several intense reflections indicated acceptable crystal quality [27b].

Data were collected for $4° \leq 2\theta \leq 50°$ (ω (Wyckoff) scans, $-21 \leq h \leq 21$, $0 \leq k \leq 18$, $0 \leq 1 \leq 30$) at 193 K. Scan width on ω was 0.60°, with a variable scan rate of 3.00–29.30° min^{-1}. Three control reflections, collected every 97 reflections, showed no significant trends. Background measurement by stationary crystal/stationary counter technique was taken at the beginning and end of each scan for half of the total scan time.

Lorentz and polarization corrections were applied to 6944 reflections. A semi-empirical absorption correction was applied (ellipsoid approximation; $\mu_{xr} = 0.03$; $T_{max} = 0.9434$, $T_{min} = 0.8983$) [27c]. A total of 6530 unique reflections ($R_{int} = 0.02$), with $|I| \geq 0.0\ \sigma I$, were used in further calculations. The structure was solved by Patterson Synthesis [27d]. Full-matrix least-squares anisotropic refinement for all non-hydrogen atoms yielded $R = 0.049$, $R_w = 0.048$ and $S = 1.77$ at convergence. Hydrogen atoms were placed in idealized positions with isotropic thermal parameters fixed at 0.08 $Å^3$. Neutral atom-scattering factors and anomalous scattering correction terms were taken from a standard source [27e]. The following atoms were found to fill their sites only partially: Cl4 and Cl5 fixed at 50%; O3W and O3W′ refined to 52% and 48%, respectively. The model, corrected for variable site occupation, was used to refine the structure to convergence. Crystal data and experimental details are provided in Table 1.

Tables of hydrogen atom coordinates and anisotropic thermal parameters have deposited at the Cambridge Crystallographic Data Centre.

Table 1
Crystallographic data and data collection parameters

	$[Rh(PTAH)_3(PTA)Cl]Cl_3 \cdot 3H_2O$ (2)
Formula	$C_{24}H_{57}N_{12}O_3P_4Cl_4Rh$
Fw	930.4
Space group	monoclinic, $C2/c$
a, Å	18.407(4)
b, Å	15.947(4)
c, Å	25.532(6)
β, deg	98.47(2)
V, $Å^3$	7413(3)
Z	8
d_{calc}, g cm^3	1.667
Abs. coeff., mm^{-1}	0.961
λ, Å	0.71073
T, K	193
Transm. coeff.	0.8983/0.9434
R [a], %	4.94
R_w [a], %	4.80

[a] $R = \Sigma||F_o| - |F_c||/\Sigma|F_o|$. $R_w = \{[\Sigma w(|F_o| - |F_c|)^2]/[\Sigma w(F_o)^2]\}^{1/2}$.

2.5. Kinetic studies of the catalytic hydrogenations with sodium formate

In a typical experiment, $RhCl(PTA)_3$ (55.2 mg) was dissolved in 5 ml of 5 M aqueous sodium formate, 1 ml of a solution 0.439 M in methyl cyclohexane in chlorobenzene, and 3.5 ml of chlorobenzene were added, and the mixture was adjusted to the appropriate temperature. After at least a 20 min induction period and when the catalyst solution had turned dark brown, *trans*-cinnamaldehyde (0.5 ml) was added. The reaction was then monitored by taking samples from the organic layer at various times and determining the extent of product formation by GC with methyl cyclohexane as an internal standard. The total volume of the organic layer was kept constant at 5 ml. (A similar method was used for determining the rates of hydrogenation and isomerization of allyl benzene). The catalyst poisoning experiments were carried out as above except that either cyclooctatetrene (5.1 equivalents) or Hg(O) (0.1 ml) was added to the catalyst solution after a 10 min induction period. This resulting solution was then stirred at 75°C for 20 min before the chlorobenzene, internal standard, and substrate were added.

2.6. Titrations of $[Rh(PTAH)(PTA)_2Cl]Cl$

Complex **1** (24 mg) was added to 20 ml of water saturated with either argon or hydrogen at the appropriate temperature. The pH was then either kept constant by the addition of 0.193 M KOH by the autoburette and titrator or the pH was allowed to change and the number of equivalents of protons liberated was determined by titrating the solution back to the initial

pH. The total number of equivalents of protons liberated was the same irrespective of whether (i) the complex was added to water under argon, allowed to reach equilibrium, and hydrogen was then bubbled through the solution or (ii) the complex was added to water under hydrogen.

2.7. Labelling experiment

Infrared spectra of 0.03 M solutions of [Rh(PTAH)$(PTA)_2Cl]Cl$ were recorded in both H_2O and $H_2{}^{18}O$. The peak assigned to the P=O stretch of 1,3,5 triaza-7-phosphaadamantane oxide (PTAO) in H_2O was shifted from 1151 cm^{-1} to 1120 cm^{-1} upon dissolution in the labelled water.

2.8. Catalyst recycling experiments

In a typical experiment, 4.9 ml of chlorobenzene were added to a solution of 46.4 mg (0.07 mmol) $RhCl(PTA)_3$ in 5 ml of 5 M aqueous NaOOCH at 70°C under nitrogen. An induction time of 15 min was allowed and then 0.095 ml (0.75 mmol) *trans*-cinnamaldehyde (0.075 ml, 0.75 mmol) was added. Samples were taken after 5, 15, 25 and 40 min, and analyzed by GC in order to determine the relative rates of reaction. After each run, 1 ml of the organic layer was extracted by syringe. The sample was evaporated to dryness and dispersed in a 0.1 M HNO_3 solution and analyzed by ICP for rhodium content. The percentage of rhodium in the aqueous layer was determined by subtracting the amount that was found to be in the total of the organic phase from that in the aqueous. The rest of the organic layer was discarded and the reaction mixture was extracted twice with 4 ml of chlorobenzene to remove any residual products or starting materials. Additional chlorobenzene and substrate were then added for the next run.

3. Results and discussion

3.1. Synthesis and reactivity of $[Rh(PTAH)(PTA)_2Cl]Cl$ (1)

The reaction of $RhCl_3$ with six equivalents of PTA in refluxing ethanol resulted in separation of a bright yellow solid, which has been formulated as [Rh(PTAH)$(PTA)_2Cl]Cl$, **1**. Although crystals of this complex have not been obtained, crystals isolated from 0.1 M HCl have been structurally characterized and shown to be $[Rh(PTAH)_2Cl_2]Cl$ [26]. The solid-state structure of this complex reveals the geometry about the rhodium(I) center to be that of a square planar anion with two *cis* chloride ligand. The phosphine ligands are monoprotonated at nitrogen and an additional chloride is present in the lattice equidistant between the phosphines to bring about charge balancing. Crystallization of **1** was complicated by the possibility of hydrolysis to form rhodium hydroxo species, which can further oligomerize or catalyze phosphine oxidation [28]. Evidence for this reaction was provided by IR, NMR, and UV-VIS spectroscopy. Infrared spectra of **1** in the solid state indicates the presence of a small amount of PTAO present as an impurity ($\nu_{(P=O)}$ 1167 cm^{-1}). However, the ^1H and ^{31}P NMR spectra of **1** within minutes of dissolution in water indicated the presence of a significant quantity of PTAO even when oxygen was carefully excluded. On changing from H_2O to $H_2{}^{18}O$ as solvent, the P=O stretch in the IR spectrum shift from 1151 cm^{-1} to 1120 cm^{-1} (calculated 1127 cm^{-1}), which is consistent with incorporation of oxygen from water into the phosphine oxide.

Reaction of the rhodium compound, **1**, with water can also be monitored by UV-VIS spectroscopy. The absorption of the broad shoulder at 374 nm observed for complex **1** decreases, and a peak grows up at 414 nm, resulting in a sharp isobestic point at 394 nm. The changes were similar but larger in sodium phosphate buffer (pH = 7). This is consistent with the occurrence of a reversible hydrolysis, which would be promoted by a more basic medium. Additionally, the dissolution of **1** in water at 20°C and 40°C results in the liberation of 1.49 mol and 1.83 mol of protons per mole of compound, respectively. One equivalent of HCl is present in the starting material, and the additional protons are derived from the reaction of **1** with water, which concomitantly affords PTAO. This reaction was inhibited by the presence of an excess of PTA, non-coordinating and coordinating acids, and hydrogen gas. In these cases only about 5% of the total phosphine was present as PTAO compared with 20% or 30% for sodium formate solutions or water, as determined by ^{31}P NMR.

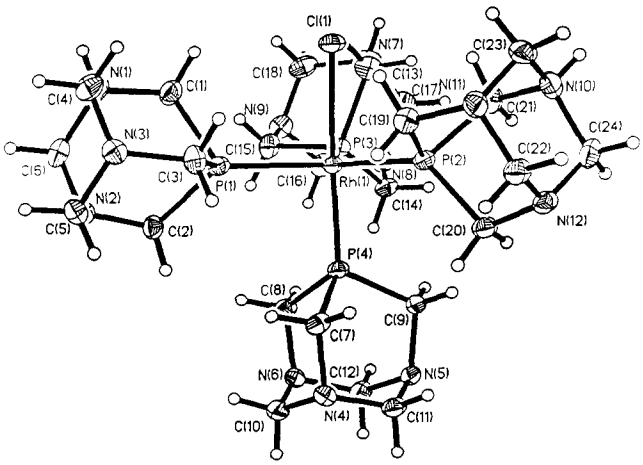

Fig. 1. ORTEP view of complex **2** with ellipsoids drawn at the 50% probability level. Protonation at nitrogen atoms, waters of hydration, and chloride ions are omitted for clarity.

Reaction 1 summarizes the behavior of complex **1** in water, and is consistent with the observations noted herein and those for the rhodium(I) tris-*m*-sulphonatophenylphosphine analog in water [28b]. That is, complex **1** oxidatively adds water to afford an hydriohydroxo rhodium(III) species, which subsequently oxidizes PTA to its oxide. The oxidation of PTA by rhodium(I) in water is inhibited in the presence of an excess of PTA because of the formation of the coordinatively saturated species, complex **2** (vide infra), and by acids, which presumably shift the equilibria to the left. In keeping with this observation, Grushin and Alper have demonstrated the pivotal role of OH^- ions in the formation of phosphine oxides from $(Ph_3P)_2PdCl_2$ in aqueous/benzene solution [29]. So far, we have not directly detected a rhodium hydride species in solution.

$$ClRh(I)(PTA)_3 \overset{H_2O}{\rightleftharpoons} ClRh(III)(H)(OH)(PTA)_3 \rightleftharpoons [HRh(I)(PTA)_2] + PTAO + HCl \quad (1)$$

3.2. Synthesis and structure of $[Rh(PTA)(PTAH)_3Cl]Cl_3$ (2)

$[Rh(PTAH)(PTA)_2Cl]Cl$ reacts with excess phosphine to give a dark-red solid, $[Rh(PTA)(PTAH)_3Cl]Cl_3$ (**2**), which has been structurally characterized by X-ray diffraction (Fig. 1). Suitable crystals were isolated from solutions of $[Rh(PTAH)(PTA)_2Cl]Cl$ in the presence of two equivalents of PTA in 0.05 M aqueous HNO_3/acetone. Final atomic coordinates for all non-hydrogen atoms are listed in Table 2. Selected bond lengths and angles are listed in Tables 3 and 4, respectively. The geometry about the rhodium(I) center is trigonal bipyramidal with the chloride in an axial position. The geometry is not consistent with the solution ^{31}P NMR spectrum for **2**, which indicates two equatorial and two axial phosphine ligands bonded to rhodium. The Rh–P equatorial bonds in **2** which average 2.32 Å, are slightly longer, by approximately 0.1 Å, than either the Rh–P axial bond or the Rh–P bonds in $[Rh(PTAH)_2Cl_2]Cl$ [26], but are quite similar to the Rh–P bonds in $[Rh(PMe_3)_4]Cl$ [30]. However, the Rh–P axial bond length in **2** of 2.206 Å is close to the lengths of the Rh–P bonds *trans* to chloride in $RhCl(PMe_3)_3$ [30] and $[Rh(PTAH)_2Cl_2]Cl$ [26] (2.203 Å and 2.188 Å, respectively). The Rh–Cl bond length is approximately 0.06 Å longer than expected by comparison with data for analogous compounds. It is interesting to note that while the bond lengths are in line with those for the PMe_3 analog, $[Rh(PMe_3)_4]Cl$, the latter displays tetrahedral geometry about the rhodium and the chloride is fully dissociated (the closest contact to Cl^- being $Cl \cdots C$ 3.90 Å) [30]. Two of the phosphines in complex **2** are slightly bent out of the equatorial plane toward the chloride in order to relieve steric crowding between PTA ligands. No $P_{ax}–Rh–P_{eq}$ bond angles are less than 90°, while one of the $P_{eq}–Rh–P_{eq}$ bond angles is compressed to 110.9°. One nitrogen (N1, N7 and

Table 2
Atomic coordinates ($\times 10^4$) and equivalent isotropic displacement parameters ($Å^2 \times 10^3$) for $C_{24}H_{57}N_{12}O_3P_4Cl_4Rh$ [a]

Atom	x	y	z	U_{eq} [b]
Rh(1)	2370(1)	5909(1)	3242(1)	15(1)
Cl(1)	2282(1)	4565(1)	2755(1)	24(1)
Cl(2)	2063(1)	743(1)	4577(1)	27(1)
Cl(3)	−295(1)	2625(1)	5044(1)	38(1)
Cl(4)	5000	3463(1)	2500	29(1)
Cl(5)	0	1955(2)	2500	209(3)
P(1)	1558(1)	5308(1)	3759(1)	18(1)
P(2)	1966(1)	6448(1)	2414(1)	17(1)
P(3)	3580(1)	5611(1)	3589(1)	18(1)
P(4)	2379(1)	7156(1)	3617(1)	17(1)
O(1W)	1182(2)	2203(2)	3685(2)	52(1)
O(2W)	1369(2)	2412(2)	4958(2)	63(2)
O(3W)	594(4)	3841(5)	2423(3)	66(3)
O(3W′)	1145(7)	2889(9)	2688(5)	124(7)
N(1)	1105(2)	3804(2)	4176(1)	24(1)
N(2)	883(2)	5076(2)	4659(1)	23(1)
N(3)	122(2)	4763(2)	3808(1)	22(1)
N(4)	1553(2)	8517(2)	3850(1)	21(1)
N(5)	2815(2)	8815(2)	3660(1)	20(1)
N(6)	2633(2)	8160(2)	4504(1)	19(1)
N(7)	4771(2)	4579(2)	3463(1)	29(1)
N(8)	5083(2)	5934(2)	3881(1)	22(1)
N(9)	4564(2)	4822(2)	4373(1)	25(1)
N(10)	2198(2)	6379(2)	1356(1)	25(1)
N(11)	925(2)	6260(2)	1515(1)	21(1)
N(12)	1538(2)	7614(2)	1603(1)	21(1)
C(1)	1694(2)	4173(3)	3897(2)	25(1)
C(2)	1430(2)	5601(3)	4447(2)	24(1)
C(3)	575(2)	5246(3)	3475(2)	22(1)
C(4)	338(2)	3901(3)	3853(2)	27(1)
C(5)	159(2)	5141(3)	4334(2)	25(1)
C(6)	1098(2)	4211(3)	4715(2)	26(1)
C(7)	1482(2)	7686(2)	3598(2)	22(1)
C(8)	2715(2)	7284(2)	4332(1)	20(1)
C(9)	2922(2)	8025(2)	3383(2)	20(1)
C(10)	1864(2)	8438(3)	4415(2)	23(1)
C(11)	2034(2)	9059(2)	3590(2)	23(1)
C(12)	3079(2)	8734(3)	4232(2)	24(1)
C(13)	4008(2)	4819(3)	3206(2)	28(1)
C(14)	4366(2)	6349(3)	3690(2)	23(1)
C(15)	3790(2)	5087(3)	4241(2)	25(1)
C(16)	5072(2)	5541(3)	4398(2)	28(1)
C(17)	5287(2)	5329(3)	3512(2)	29(1)
C(18)	4764(2)	4207(3)	4012(2)	31(1)
C(19)	1087(2)	6020(3)	2075(2)	23(1)
C(20)	1796(2)	7547(3)	2181(2)	26(1)
C(21)	2546(2)	6156(3)	1914(2)	23(1)
C(22)	848(2)	7164(3)	1450(2)	24(1)
C(23)	1460(2)	5946(3)	1211(2)	26(1)
C(24)	2081(2)	7325(3)	1298(2)	28(1)

[a] Estimated standard deviations are given in parentheses.
[b] Equivalent isotropic U defined as one third of the trace of the orthogonalized U_{ij} tensor.

Table 3
Selected bond lengths (Å) for $C_{24}H_{57}N_{12}O_3P_4Cl_4Rh$ [a]

Rh(1)–Cl(1)	2.471(1)	Rh(1)–P(1)	2.341(1)
Rh(1)–P(2)	2.301(1)	Rh(1)–P(3)	2.322(1)
Rh(1)–P(4)	2.206(1)	N(1)–C(1)	1.504(6)
N(1)–C(4)	1.535(5)	N(1)–C(6)	1.523(5)
N(2)–C(2)	1.473(5)	N(2)–C(5)	1.466(5)
N(2)–C(6)	1.435(5)	N(3)–C(3)	1.490(5)
N(3)–C(4)	1.430(5)	N(3)–C(5)	1.465(5)
N(4)–C(7)	1.472(5)	N(4)–C(10)	1.477(5)
N(4)–C(11)	1.464(5)	N(5)–C(9)	1.472(5)
N(5)–C(11)	1.475(5)	N(5)–C(12)	1.477(5)
N(6)–C(8)	1.480(5)	N(6)–C(10)	1.468(5)
N(6)–C(12)	1.470(5)	N(7)–C(13)	1.509(5)
N(7)–C(17)	1.521(5)	N(7)–C(18)	1.525(6)
N(8)–C(14)	1.493(5)	N(8)–C(16)	1.466(5)
N(8)–C(17)	1.435(6)	N(9)–C(15)	1.476(5)
N(9)–C(16)	1.474(5)	N(9)–C(18)	1.431(6)
N(10)–C(21)	1.515(5)	N(10)–C(23)	1.521(5)
N(10)–C(24)	1.527(5)	N(11)–C(19)	1.468(5)
N(11)–C(22)	1.457(5)	N(11)–C(23)	1.431(5)
N(12)–C(20)	1.487(5)	N(12)–C(22)	1.461(5)
N(12)–C(24)	1.429(6)		

[a] Estimated standard deviations are given in parentheses.

N10) of each of the three PTA ligands is protonated; this is revealed by the longer C–N bond lengths to the protonated nitrogens (1.52 Å vs. 1.46 Å). An array of electrostatic and hydrogen bonding links the discrete molecules into a complex three-dimensional network.

3.3. Catalytic hydrogenations

The features of the reduction of *trans*-cinnamaldehyde (Eq. 2) using **1** and sodium formate, as reductant, were studied. The catalyst exhibits high selectivity for reduction of the carbon–carbon double bond. This transformation is approximately two orders of magnitude more facile than the reduction of the aldehyde moiety. In contrast with our $RuCl_2(PTA)_4$ catalyst system, which is an effective catalyst for the regioselective conversion of unsaturated aldehydes to unsaturated alcohols, complex **1** selectively transfers hydrogen to the

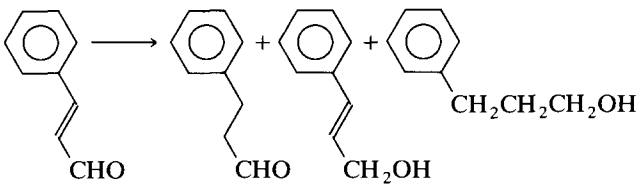

(2)

Table 4
Selected bond angles (deg) for $C_{24}H_{57}N_{12}O_3P_4Cl_4Rh$ [a]

Cl(1)–Rh(1)–P(1)	85.9(1)	Cl(1)–Rh(1)–P(2)	82.8(1)
P(1)–Rh(1)–P(2)	121.6(1)	Cl(1)–Rh(1)–P(3)	90.1(1)
P(1)–Rh(1)–P(3)	110.9(1)	P(2)–Rh(1)–P(3)	126.1(1)
Cl(1)–Rh(1)–P(4)	174.9(1)	P(1)–Rh(1)–P(4)	95.1(1)
P(2)–Rh(1)–P(4)	92.4(1)	P(3)–Rh(1)–P(4)	94.2(1)

[a] Estimated standard deviations are given in parentheses.

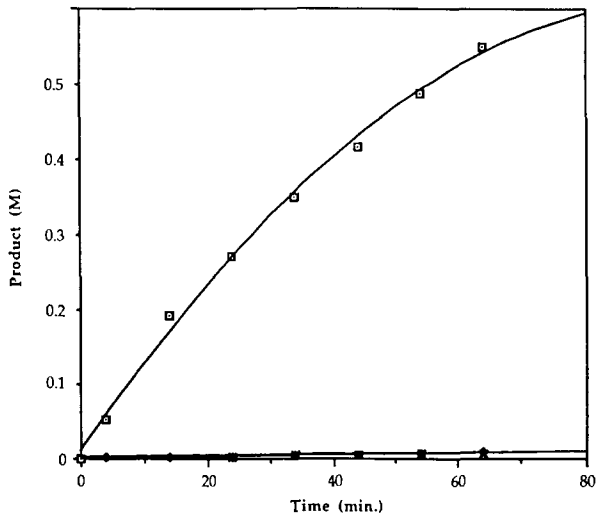

Fig. 2. Reaction profiles for the reduction of *trans*-cinnamaldehyde (0.794 M) in the presence of complex **1** with aqueous NaOOCH (5 M) at 75°C; □ hydrocinnamaldehyde, ◦ cinnamyl alcohol, + phenyl propanol.

carbon–carbon double bond [1,26]. For example, after 200 min of reaction the reduction of *trans*-cinnamaldehyde by **1** (Fig. 2) yielded 93.9% hydrocinnamaldehyde and only 3.0% and 3.1% cinnamyl alcohol and phenyl propanol, respectively. Additionally, complex **1** does not readily decarbonylate the aldehyde, in contrast to the similar Wilkinson's catalyst. Refluxing the catalyst with a large excess of neat cinnamaldehyde for several hours resulted in formation of a clear aqueous layer and the production of a water-insoluble orange oil which showed no absorptions in the metal carbonyl stretching region in the IR spectrum. GC analysis of the organic layer did not indicate the presence of a decarbonylated product.

In separate experiments involving pretreatment of the catalyst system with mercury and with cyclooctatetraene, reductions in catalytic activity were noted (see Fig. 3). Elemental mercury and cyclooctatetraene have been previously found to selectively poison heterogeneous and homogeneous catalysts, respectively [31]. These observations, coupled with corroborative results from ^{31}P NMR and UV-VIS spectroscopic (vide infra) suggest that both homogeneous and heterogeneous reaction pathways are operating. Hence, because the reaction may be in part catalyzed by bulk or finely divided metal colloids, mechanistic studies are to be complicated. Nevertheless, some observations on this biphasic hydrogenation reaction with regard to reaction rates have been noted during our studies of this process, and these are presented below.

The hydrogenation process exhibited a linear correlation between the reaction rate and the concentration of complex **1** over the concentration range studied (0.01–0.03 M) with a slope of 0.53. Below a catalyst concentration of 0.01 M the reaction displayed non-lin-

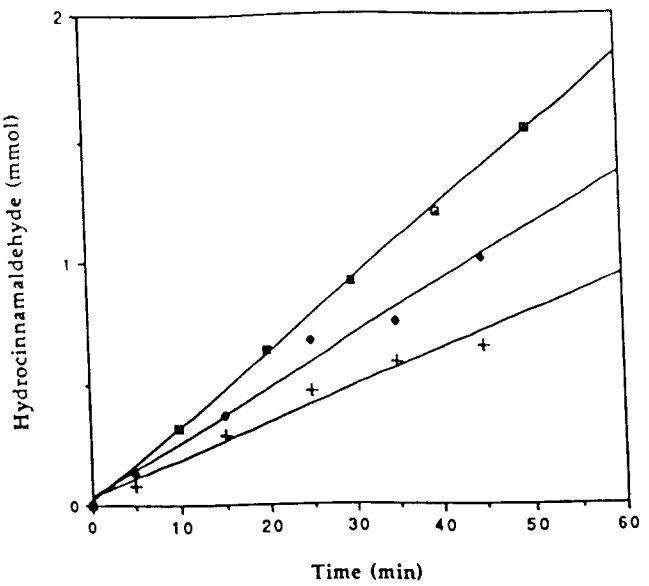

Fig. 3. Effect of pretreatment with □ nothing, ◆ cyclooctatetraene, + Hg(0), on the initial rate of reduction of *trans*-cinnamaldehyde (0.794 M) with **1** (9×10^{-5} M) with complex **1** in aqueous NaO_2CH (5 M) at 75°C.

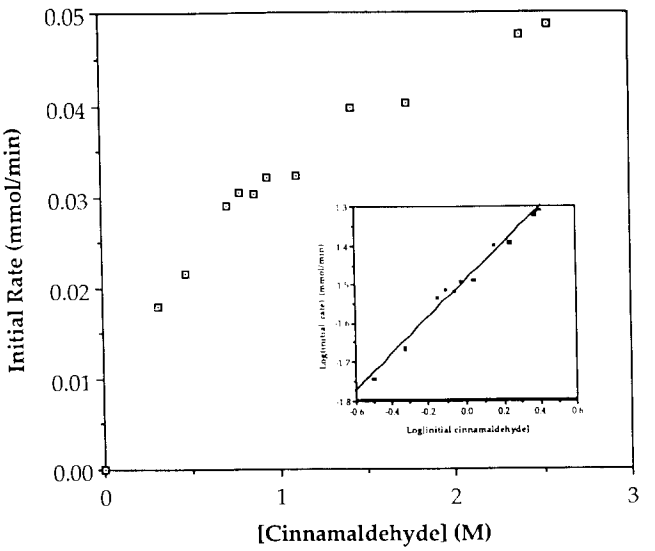

Fig. 4. Dependence of the rate on initial substrate concentration for the reduction of *trans*- cinnamaldehyde in the presence of complex **1** (9×10^{-5} M) with aqueous NaOOCH (5 M) at 75°C. The insert shows the corresponding log-log plot, which provides a reaction order of 0.47.

ear behavior, going to zero at zero catalyst concentration. The order of the reaction in substrate was mixed (about 0.5), initially exhibiting an increased rate with increasing aldehyde concentration and ultimately reaching a maximum, or approaching saturation, at [aldehyde] greater than 3 M (Fig. 4). The reaction displays a sharp rise in rate as a function of sodium formate in the less than 0.50 M range, followed by a slow decrease in rate with increasing sodium formate concentration, eventually levelling off at around 4 M. Because the reaction involves the aldehyde dissolved in the bulk aqueous phase, this behavior is probably the result of a salting-out effect at the higher electrolyte concentration. Reactions were studied at 5 M [NaOOCH] in water to ensure that formate concentration remained relatively constant for the duration of the hydrogenation. The rate was not effected by the presence of excess chloride or silver triflate, but was strongly inhibited by an excess of PTA, the reaction essentially being quenched in the presence of one equivalent excess of PTA. In accord with this observation, complex **2** is not a hydrogenation catalyst. The temperature dependence of the reaction was also determined, revealing an apparent activation energy of 18.8 kcal mol^{-1}. Additionally, this complex is easily recycled with minimal loss of activity until the fourth recycle (see Table 5); this loss in activity was shown not to involve leaching of rhodium into the organic layer.

Allylbenzene is also rapidly hydrogenated by complex **1**. The hydrogenation is accompanied by extensive isomerization of the olefinic bond to afford *cis*- and primarily *trans*-propenylbenzene (Table 6 and Fig. 5). The isomerization was more pronounced when NaOOCH was used as a hydrogen source, with which the hydrogenation reaction is somewhat slower than when hydrogen gas is used. Indeed, in this instance isomerization can be made the major reaction at ambient temperature (entry 4 in Table 6).

In an attempt to elucidate the mechanism of these hydrogenations the reaction of [Rh(PTAH)(PTA)$_2$Cl]Cl with sodium formate was studied by NMR spectroscopy. The ^{1}H and ^{31}P NMR spectra were recorded at room temperature for a sample made by dissolving complex **1** in water in the presence of an excess of sodium formate; spectra were recorded immediately after preparation and again after heating the solution until it turned dark brown. The two broad singlets in the ^{1}H NMR spectrum corresponding to [Rh(PTAH)-

Table 5
Results of recycling of [Rh(PTAH)(PTA)$_2$Cl]Cl catalyzed hydrogenations of *trans*-cinnamaldehyde

Run number	Relative rate	% Rh Aqueous [a]
1	1.000	100
2	1.027	99.61
3	1.027	98.73
4	0.719	98.29 (97.43)
1	1.000	100
2	–	99.52
3	0.683	98.90
4	0.783	98.22 (97.94)
1	1.000	100
2	0.949	99.29
3	0.925	99.11
4	0.752	98.44 (97.70)

[a] Percentages in parentheses refer to amount after run 4.

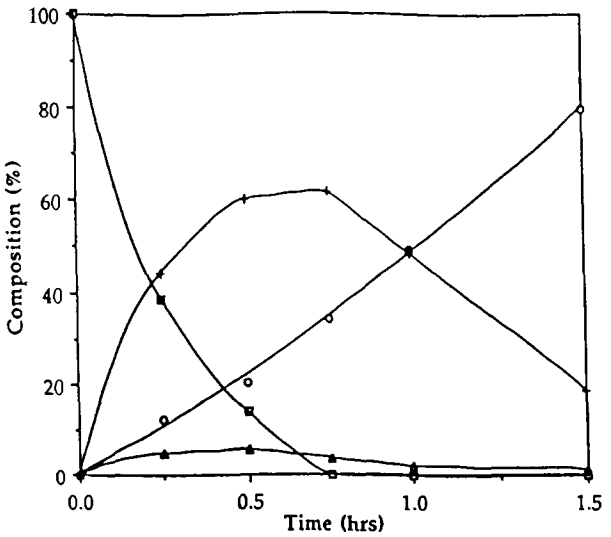

Fig. 5. Reaction profile for the reduction of allyl benzene (0.66 ml) in the presence of complex **1** (0.08 mmol) in 5 ml of 5 M formate buffer with H_2 at 50°C; □ allyl benzene, ◦ propyl benzene, + *trans*-propenyl benzene, △ *cis*-propenyl benzene.

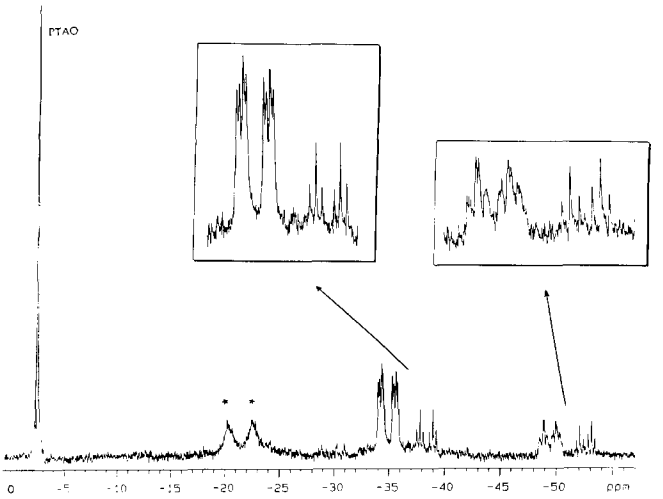

Fig. 6. ^{31}P NMR spectrum of the mixture formed in the reversible reaction of $[Rh(PTAH)(PTA)_2Cl]Cl$ with H_2. Peaks indicated by asterisks are caused by $[Rh(PTAH)(PTA)_2Cl]Cl$.

$(PTA)_2Cl]Cl$ disappeared, and the resulting spectrum showed the presence of PTAO, a quintet at 4.6 ppm and two broad singlets at 4.2 ppm and 4.1 ppm. The ^{31}P NMR spectroscopy revealed the presence of the phosphine oxide and a rhodium compound with four phosphines (−39 ppm, dt, $J_{Rh-P} = 94$ Hz, $J_{P-P} = 24$ Hz; −53 ppm, dt, $J_{Rh-P} = 85$ Hz, $J_{P-P} = 24$ Hz); however, there are several very broad regions in the baseline, probably caused by fast exchange processes. Surprisingly, the presence of 1.5 additional equivalents of PTA had no significant effect on the spectra.

Complex **1** is also active for olefin hydrogenation with hydrogen gas as a reductant. However, because the reaction rates with dihydrogen are limited by the slow transfer of H_2 between the two phases, it is often necessary to enhance the rate of the reaction by use of a cosolvent. Hence, for measurement of the rate of hydrogenation of cinnamaldehyde under biphasic conditions with dihydrogen ethanol was used as a cosolvent. Initial efforts at optimization of this process gave turnover numbers in the region of 250 h^{-1} at 78°C. Attempts to observe an intermediate hydride formed by the reaction of complex **1** with dihydrogen by ^1H NMR spectroscopy were also unsuccessful, even under conditions involving use of high pressure (1000 psi), slightly reduced temperatures, and cosolvent mixtures aimed at increasing the solubility of H_2. The ^1H NMR spectra were not very informative because of the presence of very broad, overlapping peaks at 4–4.8 ppm. However, in the reaction of $Rh(PTA)_3Cl$ with hydrogen gas, the ^{31}P NMR spectrum (Fig. 6) showed in addition to signals from unchanged starting material and PTA oxide, two overlapping double doublets at −34.8 ppm ($J_{Rh-P} = 104.5$ Hz, $J_{P-P} = 26$ Hz) and −35.0 ppm ($J_{Rh-P} = 105.4$ Hz, $J_{P-P} = 26$ Hz) and two overlapping double triplets at −49.3 ppm ($J_{Rh-P} = 90.9$ Hz, $J_{P-P} = 26$ Hz) and −49.4 ppm ($J_{Rh-P} = 89.9$ Hz, $J_{P-P} = 26$ Hz) in a ratio of 2:1 (**6a**, **6b**), and two

Table 6
Reduction of allylbenzene by $[Rh(PTAH)(PTA)_2Cl]Cl$ [a]

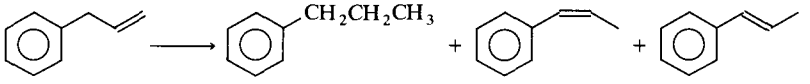

	3	**4**	**5**		
Temp. (°C)	Time (hrs)	Reducing agent	**3** [d]	**4**	**5**
50	1.75	H_2 [b]	50.6	2.0	44.5
50	3	H_2 [c]	3.7	4.3	7.7
50	3	NaOOCH	11.6	5.2	66.1
25	8	NaOOCH	3.0	3.6	60.8

[a] 0.082 mmol of **1**, 5.0 mmol of neat allylbenzene, 5 ml of 5 M NaOOCH, *or*
[b] 0.08 M sodium phosphate buffer, *or*
[c] 0.1 M HCl.
[d] G.C. yields.

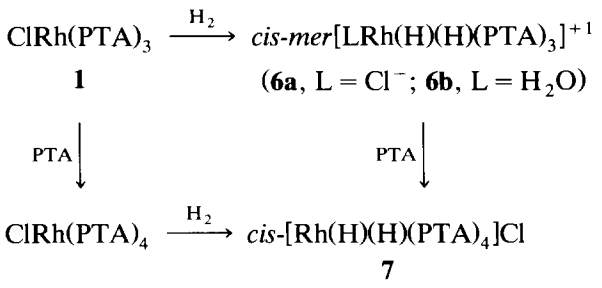

Scheme 1.

doublets of triplets in a 1:1 ratio at −38.9 ppm and −52.5 ppm (**7**) (see Scheme 1). When nitrogen was bubbled through the solution, the overlapping doublets of triplets and doublets disappeared and the peaks corresponding to the starting material and PTAO increased in intensity. When the yellow solution of **1** was heated at 35°C under H_2 it became dark, and the reaction between the starting material and hydrogen went to completion. The reaction of **1** with H_2 is much simpler in the presence of a non-coordinating acid. The ^{31}P NMR spectrum shows only the signals from PTAO, a doublet of doublets at −31 ppm and a doublet of triplets at −45 ppm (**6a** or **6b**). As indicated in Scheme 1, complex **2** also reacts with dihydrogen to afford the same species **7** as was produced from the reaction of complex **1** with dihydrogen in the presence of an excess of PTA. However, this complex is not an active hydrogenation catalyst.

The reaction of complex **1** with H_2 at 40°C results in the production of 0.4 equivalents of protons, in addition to the protons liberated in the reaction of the catalyst with water. This reaction can also be monitored by UV-VIS spectroscopy. Under a variety of conditions bubbling of hydrogen through an aqueous catalyst solution results in an overall increase in absorption and a loss of spectral features. This would seem to indicate the formation of oligomers or colloids. The production of protons during this process can proceed by several pathways. For instance, a dihydride species formed by oxidative addition of H_2 can be subsequently partially deprotonated, a concerted reaction can occur between complex **1** and H_2 to produce $HRh(I)(PTA)_3$ and HCl, or a Rh(I)(OH)PTA species can react with H_2 in either a concerted or step-wise fashion. As yet our experimental observations cannot distinguish between these and other mechanisms. This is in contrast with the situation for the Rh–TPPTS system [32] for which Laghmari and Sinou found that isotope incorporation into the substrate occurs only after insertion of the first hydrogen into the substrate, and this can occur by protonolysis of the carbon–rhodium bond of an intermediate σ–rhodium complex or by H/D exchange in the coordination sphere of the same complex. The facile deprotonation/exchange of complex **1** under hydrogen with water accounts for our inability to observe the hydride by ^1H NMR spectroscopy and implies that, in our case, homogeneous hydrogenation could be occurring either via a dihydride or monohydride mechanism, or both.

4. Concluding remarks

The results described herein further illustrate the potential utility of water-soluble catalysts derived from the small, basic and air-stable 1,3,5-triaza-7-phosphaadamantane ligand in biphasic processes. In this instance $[Rh(PTAH)(PTA)_2Cl]Cl$ serves as an effective catalyst for the regioselective hydrogenation of α,β-unsaturated aldehydes to give saturated aldehydes with either dihydrogen or NaOOCH as reductant, and without concomitant decarbonylation. Furthermore, it is shown that this catalyst system can be easily and efficiently recycled. However, use of water as a solvent has important implications for the mechanism of hydrogenations, and it is not always possible to assume that the mechanism operating for a homogeneous catalyst in organic solvents is applicable to its water soluble analogue. Indeed there are significant differences between various water soluble catalysts; e.g., we observe oxidation of PTA to PTAO in reactions with water under hydrogenation conditions. This is in contrast to the observations on the closely related Rh–TPPTS system, for which no TPPTS oxide is observed in reaction mixtures after hydrogenation [16d]. Although we have not been able to define the detailed mechanistic aspects of this complicated hydrogenation process satisfactorily, many of the reaction variables have been described.

Acknowledgements

The financial support of this research by the National Science Foundation (Grants CHE91-19737 and INT90-08227) and the Hungarian Academy of Science (30,008/134/90) and the Hungarian National Research Foundation (OTKA 1699) is greatly appreciated. The assistance of Dr. Agnes Kathó in some experiments is gratefully acknowledged.

References and notes

[1] D.J. Darensbourg, F. Joó, M. Kannisto, A. Kathó, J.H. Reibenspies and D.J. Daigle, *Inorg. Chem. 33* (1994), 200.
[2] G.W. Parshall and S.D. Ittel, *Homogeneous Catalysis*, 2nd Ed., John Wiley, New York 1992.
[3] (a) Z.M. Michalska and D.E. Webster, *Platinum Metals Rev., 18 (2)* (1974) 65; (b) F.R. Hartley, *Supported Metal Complexes: A New Generation of Catalysts*, Kluwer Academic Publishers, Boston, 1985.

[4] (a) E.G. Kuntz, *Chemtech*, (1987) 570; (b) H. Bahrmann and H. Bach, *Phosphorous and Sulfur*, *30* (1987) 611.
[5] (a) I.T. Horvath, *Catal. Lett.*, *6* (1990) 43; (b) I. Toth, B.E. Hanson and M.E. Davis, *J. Organomet. Chem.*, *397* (1990) 109; (c) J.P. Arhancet, M.E. Davis, J.S. Merola and B.E. Hanson, *J. Catal.*, *121* (1990) 327. (d) F. Sánchez, M. Iglesias, A. Corma and C. del Pino, *J. Mol. Catal. 70* (1991) 369; (e) M.E. Davis, *Chemtech*, (1992) 498.
[6] (a) G. Schmid and A. Lehnert, *Angew. Chem. 101* (1989) 773; (b) C. Larpent and H. Patin, *J. Mol. Catal.*, *61* (1990) 65; (c) C. Larpent, F. Brisse-Le Menn and H. Patin, *J. Mol. Catal.*, *65* (1991) L35.
[7] (a) F. Joó and Z. Toth, *J. Mol. Catal.*, *8* (1980) 369; (b) P. Kalck and F. Monteil, *Adv. Organometal. Chem.*, *34* (1992) 219; (c) M.J.H. Russell, *Platinum Metals Rev.*, *32 (4)* (1988) 179; (d) A. Bényei and F. Joó *J. Mol. Catal. 58* (1990) 151.
[8] R.H. Crabtree, M.F. Mellea, J.M. Mihelcic and J.M. Quirk, *J. Am. Chem. Soc.*, *104* (1982) 107.
[9] (a) H. Müller, C. Opitz and L. Skala, *J. Mol. Catal. 54* (1989) 389; (b) A. Henglein, *Chem. Rev.*, *89* (1989) 1861; (c) H. Hirai, M. Ohtaki and M. Komiyama *Chem. Lett.*, (1986) 269. (d) H. Hirai, M. Ohtaki and M. Komiyama, *Chem. Lett.*, (1987) 149; (e) M. Boutonnet, J. Kizling, V. Mintsa-Eya, A. Choplin and R. Touroude, G. Maire and P. Stenius, *J. Catal.*, *103* (1987) 95; (f) K. Kuriha and J.H. Fendler, *J. Am. Chem. Soc. 105* (1983) 6152.
[10] (a) Y. Wang, H. Liu and Y. Jiang, *J. Chem. Soc., Chem. Comm.*, (1989) 1878; (b) Y. Nakao and K. Kaeriyama, *J. Colloid Interface Sci. 131* (1989) 186; (c) M. Ohtaki, N. Toshima, M. Komiyama and H. Hirai, *Bull. Chem. Soc. Jpn.*, *63* (1990), 1433.
[11] P.A. Chaloner, M.A. Esteruelas, F. Joó and L.A. Oro, *Homogeneous Hydrogenation*, Kluwer Academic Publishers, Dordrecht, Netherlands, 1993, Ch. 5, and references therein.
[12] Ch. Elschenbroich and A. Salzer, *Organometallics: A Concise Introduction*, 2nd Ed., VCH Verlagsgesellschaft, Weinheim, 1992.
[13] (a) E. Fache, C. Santini, F. Senocq and J.M. Basset, *J. Mol. Catal.*, *72* (1992) 337; (b) E. Fache, F. Senocq, C. Santini and J.M. Basset, *J. Chem. Soc., Chem. Comm.*, (1990) 1776.
[14] J. Falbe, *New Syntheses with Carbon Monoxide*, Springer, New York, 1980.
[15] W.A. Hermann, J.A. Kulpe, J. Kellner, H. Riepl, H. Bahrmann and W. Konkol, *Angew. Chem., Int. Ed. Engl.*, *29* (1990) 391.
[16] (a) Y. Dror and J. Manassen, *J. Mol. Catal.*, *2* (1977) 219; (b) R.G. Nuzzo, D. Feitler and G.M. Whitesides, *J. Am. Chem. Soc.*, *101* (1979) 3683; (c) Willner and R. Maidan, *J. Chem. Soc., Chem. Comm.*, (1988) 876; (d) J.M. Grosselin, C. Mercier, G. Allmang and F. Grass, *Organometallics*, *10 (7)* (1991), 2126; (e) F. Joó, and E. Trócsanyi, *J. Organomet. Chem.*, *231* (1982) 63.
[17] (a) T. Okano, Y. Moriyama, H. Konishi and J. Kiji, *Chem. Lett.*, (1986) 1463; (b) J. Kiji, T. Okano, W. Nishiumi and H. Konishi, *Chem. Lett.*, (1988) 957.
[18] G. Mignani, D. Morel and Y. Colleuille, *Tetrahedron Lett.*, *26* (1985) 6337.
[19] (a) Y. Amrani and D. Sinou, *J. Mol. Catal.*, *24* (1984) 231; (b) D. Sinou and Y. Amrani, *J. Mol. Catal.*, *36* (1986) 319; (c) Y. Amrani, L. Lecomte, D. Sinou, J. Bakos, I. Toth and B. Heil, *Organometallics*, *8* (1989) 542; (d) I. Toth, B. Hanson and M.E. Davis, *Catal. Lett.*, *5* (1990) 183.
[20] (a) C. Vigo, F.M. Goni, P.J. Quinn and D. Chapman, *Biochim. Biophys. Acta*, *508* (1978) 1; (b) T.D. Madden, W.E. Peel, P.J. Quinn and D.J. Chapman, *Biochem. Biophys. Methods*, *2* (1980), 19; (c) F. Joó, N. Balogh, L.I. Horvath, G. Filep, I. Horvath and L. Vigh, *Anal. Biochem.*, *194* (1991) 34; (d) P.J. Quinn, F. Joó and L. Vigh, *Prog. Biophys. Molec. Biol.*, *53* (1989) 71.
[21] I. Willner, R. Maidan and M. Shapiro, *J. Chem. Soc., Perkin Trans., II* (1990) 559.
[22] A.A. Chachoyan and L.I. Sagradyan, *Biol. Zh. Arm.*, *40* (1987) 399.
[23] D.J. Daigle, A.B. Jr. Pepperman and S.L. Vail, *J. Heter. Chem. 112* (1974) 407.
[24] (a) M.Y. Darensbourg and D. Daigle, *Inorg. Chem.*, *14* (1975) 1217; (b) J.R. DeLerno, L.M. Trefonas, M.Y. Darensbourg, and R.J. Majeste, *Inorg. Chem.*, *15* (1976) 816; (c) D.J. Darensbourg and A.H. Graves, *Inorg. Chem. 18* (1979) 1257.
[25] E.C. Alyea, K.J. Fisher, and S. Johnson, *Can. J. Chem.*, *67* (1989) 1319.
[26] D.J. Darensbourg, F. Joó, M. Kannisto, A. Katho and J.H. Reibenspies, *Organometallics 11* (1992) 1990.
[27] (a) Control software, P3VAX 3.42 was supplied by Nicolet Analytical X-ray Instruments, Madison, WI; (b) ω scans were recorded graphically for several intense reflections, along each principle axis. Crystal quality was determined by inspection of the peak profiles and their spread in ω; (c) Several reflections were measured at intervals of ψ (the azimuthal angle corresponding to 360° rotation of the crystal about its diffraction vector). These reflections were then used to apply a semi-empirical absorption correction (XEMP) to the remaining reflections; (d) All crystallographic calculations were performed with SHELXTL-PLUS rev 3.4; (e) J.A. Ibers and W.S. Hamilton (eds.), *International Tables for X-ray Crystallography*, Kynoch Press, Birmingham, England, 1974, Vol. IV.
[28] (a) C. Larpent, R. Dabard and H. Patin, *Inorg. Chem.*, *26* (1987) 2922; (b) C. Larpent, R. Dabard and H. Patin, *Nouv. J. Chim.*, *12* (1988) 907.
[29] V.V. Grushin and H. Alper, *Organometallics 12* (1993) 1890.
[30] R.A. Jones, F.M. Real, G. Wilkinson, A.M. Galas, M.B. Hursthouse, and K.M.A. Malik, *J. Chem. Soc., Dalton Trans.*, (1980) 511.
[31] (a) D.R. Anton and R.H. Crabtree, *Organometallics*, *2* (1983) 855; (b) G.M. Whitesides, M. Hackett, R.L. Brainard, J.P.M. Lavalleye, A.F. Sowinski, A.N. Izumi, S.S. Moore, D.W. Brown and E.M. Staudt, *Organometallics*, *4* (1985) 1819; (c) S.G. Harsy, *Tetrahedron 46* (1990) 7403.
[32] M. Laghmari and D. Sinou, *J. Mol. Catal.*, *66* (1991) L15.